

A NOVEL APPROACH TO UNDERSTANDING COVID-19: EXPLORING THE INTERPLAY OF SARS-COV-2 AND CTL RESPONSE

JOÃO P.S. MAURÍCIO DE CARVALHO^{*1,2}

*jocarvalho@fc.up.pt

¹FACULTY OF SCIENCES, UNIVERSITY OF PORTO,
RUA DO CAMPO ALEGRE S/N, PORTO 4169-007, PORTUGAL

²CENTRE FOR MATHEMATICS, UNIVERSITY OF PORTO,
RUA DO CAMPO ALEGRE S/N, PORTO 4169-007, PORTUGAL

ABSTRACT. Facing a global challenge with over 6.9 million fatalities, severe acute respiratory syndrome coronavirus 2 (SARS-CoV-2), the causative agent of CoViD-19, demands novel and comprehensive approaches to understand its complex dynamics. This paper introduces a non-integer order model, capturing the intricate interplay between SARS-CoV-2 and the host's cytotoxic T lymphocytes (CTLs) response. Our work reveals a unique parameter space, in which an endemic state of SARS-CoV-2 and a CTL response-free equilibrium can coexist – a crucial finding in our quest to decipher this pervasive virus. We further explore the basic reproduction number, assessing how different model parameters can potentially inhibit or fuel the infection's progression. Through extensive numerical simulations, we scrutinize the impact of varying the order of the fractional derivative and employing diverse CTL proliferation functions. This study significantly enriches our understanding of CoViD-19 immunopathology, offering invaluable insights that could guide future research and therapeutic strategies.

1. INTRODUCTION

The first official case of CoViD-19 in China emerged in December 2019 and it was associated with the Huanan seafood market, in Wuhan [1]. Since then SARS-CoV-2 has reached 231 countries and territories having infected more than 765 million people, thus becoming a global pandemic and causing more than 6.9 million deaths worldwide [2, 3, 4]. The most frequently noticed symptoms in infected people are fever, cough and respiratory disorders [2, 5]. The most affected people are elderly and adults over 60 years old and/or those with comorbidities, such as obesity, diabetes, oncological diseases, heart problems, among others [6, 7, 8].

Today, about three years after the first outbreak, there are already several vaccines that prevent coronavirus infection. Unfortunately vaccines are still not a fast enough method to fight the pandemic, especially in economically low-income countries [9, 10]. Furthermore, the period of immunity that vaccines confer on people is not yet known

Date: June 5, 2023.

2010 Mathematics Subject Classification. 37N25, 65L15, 92B05, 92B99.

Key words and phrases. SARS-CoV-2, Immune response, Basic reproduction number, Fractional calculus, Epidemic model.

JPSMC was supported by CMUP, Portugal (UIDP/MAT/00144/2020), which is funded by Fundação para a Ciência e a Tecnologia (FCT).

*Corresponding author.

exactly. As a consequence, an increase in the number of infected people has occurred in some countries with a large percentage of vaccinated individuals [11].

It is becoming increasingly important to try to understand how the immune system reacts to SARS-CoV-2 in order to find alternatives while non-priority, young and economically disadvantaged people are not vaccinated [2, 12, 13]. Many mathematicians have proposed several models describing the dynamics of CoViD-19 in the population [14, 15, 16, 17, 18]. However, as far as mathematical modelling is concerned, existing studies on dynamical systems involving SARS-CoV-2 and the immune system have not yet been very thorough. Wang *et al.* [19] developed a mathematical model to understand the dynamics and impact that SARS-CoV-2 has on target cells and on the body's immune response. The numerical results of this model allowed the authors to conclude that anti-inflammatory treatments are an asset in the recovery of infected individuals. In addition, this type of treatment helps to decrease the viral load, especially when it reaches its peak. The same results were obtained when the treatment involved antiviral drugs. Chatterjee *et al.* [20] designed a mathematical model in order to analyse how a certain drug administered at regular intervals helps the recovery of infected individuals. The authors concluded that if the drug is applied in the right dosage and adjusted to each individual's condition, it is effective in combating SARS-CoV-2. Also, Bairagi *et al.* [21] proposed a model for the dynamics of the immune response to an infection. The authors formulated four functions to model the immune response:

$$f_1(I, C) = qIC$$

“CTL proliferation depends both on infected cells density and CTL population”;

$$f_2(I, C) = qI$$

“CTL production is assumed to depend on infected cells density only”;

$$f_3(I, C) = \frac{qIC}{\varepsilon C + 1}$$

“CTL expansion saturates as the number of CTL grows to relatively high numbers. The level at which CTL expansion saturates is expressed in the parameter ε ”;

$$f_4(I, C) = \frac{qI}{a + \varepsilon I}$$

“saturated type CTL production rate”, where a is the half-saturation constant,

and $I(t)$ and $C(t)$ represent the population of infected cells and CTL, respectively. The proliferation rate of CTL is given by q . In this paper, we will analyse f_1 , f_2 , f_3 and f_4 adapted to SARS-CoV-2 infection dynamics and we will call them *CTL proliferation functions*.

Advantages of fractional order models. Fractional order (FO) models have been increasingly used and consulted in the literature in recent years due to their capacity in describing non-linear dynamics [22, 23, 24]. These models have a great advantage over models of integer order equations since non-integer order models take into account a larger number of degrees of freedom. As such, the understanding about their dynamics and behaviours becomes more realistic. In recent times, there has been a growing interest to model epidemiological systems via non-integer order equations and in the last two and a half years, by virtue of circumstances, this interest has intensified in modelling CoViD-19 [25, 26, 27].

Model development and goals. Motivated by all the reasons mentioned above, we built a FO model for the dynamics of SARS-CoV-2 in the presence of the immune response modelled by four CTL proliferation functions. This work has three main goals: (i) to examine the role of the order of fractional derivative α , on the efficacy of the immune response, (ii) to explore the immune response for distinct CTL proliferation functions and α values, in the presence of SARS-CoV-2, (iii) find a space of parameters for which a SARS-CoV-2 endemic and a CTL response-free equilibria can coexist. In (ii), the numerical simulations of the model were obtained through the subroutine developed by Diethelm and Freed (1999) in [28]. A huge advantage of machine language is that it allows us to obtain numerical solutions very close to the real solutions, which are often extremely difficult or even impossible to obtain analytically. However, numerical methods always give us approximate solutions and not exact ones, since there is an error associated with each iteration.

Scope and adaptability of the model. While the specific focus of this study is the SARS-CoV-2 virus, with model parameters chosen accordingly, it's important to note that the structure and methodologies of the model are not exclusive to this particular pathogen. Our model could feasibly be adapted to analyse other viral infections by adjusting the relevant parameters. Thus, this model can serve as a *toy model*, providing a flexible framework for understanding the interactions between host immune responses and a variety of viral pathogens, not limited to SARS-CoV-2.

Structure. In Section 2 we describe the proposed model and analyse some of its properties. In Section 3 we computed the equilibria of the model, studied the *basic reproduction number* \mathcal{R}_0 , and found a parameter space for which a SARS-CoV-2 endemic and a CTL response-free equilibria can coexist. In Section 4 we outline some simulations of our dynamical system for different parameter values and for four proliferation functions. Finally, in Section 5 we draw the conclusions about our work.

2. THE MODEL

We analyse a FO model subdivided into four compartments: target/healthy cells susceptible to infection $T(t)$, infected cells $I(t)$, SARS-CoV-2 $V(t)$, and CTL $C(t)$ (see Table 1). Let

$$\Lambda = \{(\lambda, \beta, \mu, k, \delta, N, c, q, \sigma, \varepsilon, a) \in (\mathbb{R}^+)^{11}\}$$

be the set of parameters of our model. The proliferation rate of healthy cells is given by λ^α . Healthy cells are infected by the virus at a rate β^α . The natural death rate of healthy and infected cells are given by μ^α and δ^α , respectively. The term $N\delta^\alpha I$ represents the production of new viruses by infected cells during their lifetime. The viruses are cleared from the body at a rate of c^α . CTL are produced through the proliferation functions $f_n(I, C)$, where $f_1 = q^\alpha IC$, $f_2 = q^\alpha I$, $f_3 = q^\alpha IC/(\varepsilon C + 1)$ and $f_4 = q^\alpha I/(a + \varepsilon I)$ [21]. We consider q^α to be the proliferation rate of CTL. The level of saturation of CTL expansion is given by ε^α . Parameter a^α is the half-saturation constant. The natural death rate of CTL is given by σ^α . Also, $0 < \alpha \leq 1$ is the order of the fractional derivative. The description and value of these parameters can be found in Table 2. The system of FO equations is

$$\begin{aligned}
\frac{d^\alpha T}{dt^\alpha} &= \lambda^\alpha - \beta^\alpha VT - \mu^\alpha T \\
\frac{d^\alpha I}{dt^\alpha} &= \beta^\alpha VT - k^\alpha IC - \delta^\alpha I \\
\frac{d^\alpha V}{dt^\alpha} &= N\delta^\alpha I - c^\alpha V \\
\frac{d^\alpha C}{dt^\alpha} &= f_n(I, C) - \sigma^\alpha C.
\end{aligned} \tag{1}$$

We apply the principle of a FO derivative proposed by Caputo, *i.e.*

$$\frac{d^\alpha y(t)}{dt^\alpha} = I^{p-\alpha} y^{(p)}(t), \quad t > 0,$$

where $p = [\alpha]$ is the α -value rounded up to the nearest integer, $y^{(p)}$ is the p -th derivative of $y(r)$ and I^{p_1} is the Riemann-Liouville operator (Please see [29] and references therein)

$$I^{p_1} z(t) = \frac{1}{\Gamma(p_1)} \int_0^t (t-t')^{p_1-1} z(t') dt',$$

where $\Gamma(\cdot)$ is the gamma function.

Variable	Symbol
Target cells	$T(t)$
Infected cells	$I(t)$
SARS-CoV-2	$V(t)$
CTL	$C(t)$

TABLE 1. Description of the variables of model (1).

2.1. Model properties analysis. The solutions of the system (1) remain non-negative for the entire domain, $t > 0$. Let $\mathbb{R}_+^4 = \{x \in \mathbb{R}^4 \mid x \geq 0\}$ and $x(t) = [T(t), I(t), V(t), C(t)]^T$. First, we quote the following Generalized Mean Value Theorem [30] and corollary.

Lemma 1. [30] *Assume $f(x) \in C[a, b]$ and $D_a^\alpha f(x) \in C[a, b]$, where $0 < \alpha \leq 1$. Thus*

$$f(x) = f(a) + \frac{1}{\Gamma(\alpha)} (D_a^\alpha f)(\varepsilon) \cdot (x - a)^\alpha$$

for $a \leq \varepsilon \leq x, \forall x \in (a, b]$.

Corollary 1. *Suppose that $f(x) \in C[a, b]$ and $D_a^\alpha f(x) \in C(a, b)$, for $0 < \alpha \leq 1$.*

(1) *If $D_a^\alpha f(x) \geq 0, \forall x \in (a, b)$, then $f(x)$ is non-decreasing for each $x \in [a, b]$;*

(2) *If $D_a^\alpha f(x) \leq 0, \forall x \in (a, b)$, then $f(x)$ is non-increasing for each $x \in [a, b]$.*

This proves the main theorem.

Theorem 1. *There is a solution $x(t) = [T(t), I(t), V(t), C(t)]^T$ to the system (1) in the entire domain ($t \geq 0$) and it is unique. Furthermore, the solution remains in \mathbb{R}_+^4 .*

Proof. In [31, Theorem 3.1, Remark 3.2], we can observe that the solution of the initial value problem exists and is unique in \mathbb{R}_0^+ . To this end, it is enough to prove that the non-negative orthant \mathbb{R}_+^4 is positively invariant. So, we have to demonstrate that the vector field points to \mathbb{R}_+^4 in each hyperplane, thus limiting the non-negative orthant. Hence, for model (1), we get:

$$\begin{aligned}\frac{d^\alpha T}{dt^\alpha} \Big|_{T=0} &= \lambda^\alpha \geq 0 \\ \frac{d^\alpha I}{dt^\alpha} \Big|_{I=0} &= \beta^\alpha VT \geq 0 \\ \frac{d^\alpha V}{dt^\alpha} \Big|_{V=0} &= N\delta^\alpha I \geq 0 \\ \frac{d^\alpha C}{dt^\alpha} \Big|_{C=0} &= f_n(I, C) \geq 0.\end{aligned}$$

We concluded, by (1) of Corollary 1, that the solution will remain in \mathbb{R}_+^4 . \square

3. EQUILIBRIA AND BASIC REPRODUCTION NUMBER

Throughout this section, we will be using $f_n(I, C) = f_1(I, C)$. We will study the following equilibria of the model (1): (i) disease-free equilibrium point; (ii) CTL response-free equilibrium point; (iii) SARS-CoV-2 endemic equilibrium point and compute the *basic reproduction number*. Furthermore, we will find a space of parameters for which a SARS-CoV-2 endemic and a CTL response-free equilibria can coexist.

3.1. Disease-free equilibria. A disease-free equilibrium point of the model (1) is obtained via imposing $I = V = C = 0$. Let

$$X_0 = (T_0, I_0, V_0, C_0) = \left(\frac{\lambda^\alpha}{\mu^\alpha}, 0, 0, 0 \right).$$

be the disease-free equilibrium point where there is no infection present in the organism. The linearization matrix of (1) at a general point $X = (T, I, V, C) \in (\mathbb{R}_0^+)^4$ is given by:

$$J(X) = \begin{pmatrix} -(\beta^\alpha V + \mu^\alpha) & 0 & -\beta^\alpha T & 0 \\ \beta^\alpha V & -(k^\alpha C + \delta^\alpha) & \beta^\alpha T & -k^\alpha I \\ 0 & N\delta^\alpha & -c^\alpha & 0 \\ 0 & q^\alpha C & 0 & q^\alpha I - \sigma^\alpha \end{pmatrix}. \quad (2)$$

3.2. Basic reproduction number. In a cellular scenario, the *basic reproduction number* \mathcal{R}_0 , is the number of secondary infections due to a single infected cell in a susceptible healthy cell population [32]. Through [32, Lemma 1] the *basic reproduction number* can be obtained by the following expression:

$$\mathcal{R}_0 = \rho(FV^{-1}), \quad (3)$$

where F is the matrix of the new infection terms, V is the matrix of the remaining terms and ρ is the spectral radius of the matrix FV^{-1} . For the model (1) we get:

$$F = \begin{pmatrix} 0 & \beta^\alpha T_0 \\ 0 & 0 \end{pmatrix}, \quad V = \begin{pmatrix} \delta^\alpha & 0 \\ -N\delta^\alpha & c^\alpha \end{pmatrix}.$$

Then, using (3) we compute \mathcal{R}_0 as:

$$\mathcal{R}_0 = \frac{\beta^\alpha T_0 N \delta^\alpha}{(k^\alpha C_0 + \delta^\alpha) c^\alpha} = \frac{\beta^\alpha \lambda^\alpha}{\mu^\alpha c^\alpha} N. \quad (4)$$

3.3. Stability of the disease-free equilibrium X_0 . We are now able to understand the asymptotic behaviour of X_0 by relating it to the *basic reproduction number* \mathcal{R}_0 . By Theorem 2 of [32] we obtain Lemma 2.

Lemma 2. *If $\mathcal{R}_0 < 1$, then the disease-free equilibrium point X_0 is locally asymptotically stable. If $\mathcal{R}_0 > 1$, then X_0 is unstable.*

Proof. We know that at the disease-free equilibrium point X_0 , the matrix (2) takes the following form:

$$J(E) = \begin{pmatrix} -\mu^\alpha & 0 & -\frac{\beta^\alpha \lambda^\alpha}{\mu^\alpha} & 0 \\ 0 & -\delta^\alpha & \frac{\beta^\alpha \lambda^\alpha}{\mu^\alpha} & 0 \\ 0 & N\delta^\alpha & -c^\alpha & 0 \\ 0 & 0 & 0 & -\sigma^\alpha \end{pmatrix}, \quad (5)$$

and its eigenvalues are given by:

$$\gamma_1 = -\sigma^\alpha, \quad \gamma_2 = -\mu^\alpha,$$

$$\gamma_3 = \frac{-\mu^\alpha (c^\alpha + \delta^\alpha) + \sqrt{4N\beta^\alpha \delta^\alpha \lambda^\alpha \mu^\alpha + (c^\alpha \mu^\alpha)^2 - 2c^\alpha \mu^{2\alpha} \delta^\alpha + (\delta^\alpha \mu^\alpha)^2}}{2\mu^\alpha},$$

and

$$\gamma_4 = \frac{-\mu^\alpha (c^\alpha + \delta^\alpha) - \sqrt{4N\beta^\alpha \delta^\alpha \lambda^\alpha \mu^\alpha + (c^\alpha \mu^\alpha)^2 - 2c^\alpha \mu^{2\alpha} \delta^\alpha + (\delta^\alpha \mu^\alpha)^2}}{2\mu^\alpha}.$$

It is easy to verify that $\gamma_1 < 0$, $\gamma_2 < 0$ and $\gamma_4 < 0$. If

$$\begin{aligned}
& \gamma_3 < 0 \\
& \Leftrightarrow -\mu^\alpha (c^\alpha + \delta^\alpha) + \sqrt{4N\beta^\alpha \delta^\alpha \lambda^\alpha \mu^\alpha + (c^\alpha \mu^\alpha)^2 - 2c^\alpha \mu^{2\alpha} \delta^\alpha + (\delta^\alpha \mu^\alpha)^2} < 0 \\
& \Leftrightarrow 4N\beta^\alpha \delta^\alpha \lambda^\alpha \mu^\alpha + (c^\alpha \mu^\alpha)^2 - 2c^\alpha \mu^{2\alpha} \delta^\alpha + (\delta^\alpha \mu^\alpha)^2 < (c^\alpha \mu^\alpha)^2 + 2c^\alpha \mu^{2\alpha} \delta^\alpha + (\delta^\alpha \mu^\alpha)^2 \\
& \Leftrightarrow 4N\beta^\alpha \delta^\alpha \lambda^\alpha \mu^\alpha - 4c^\alpha \mu^{2\alpha} \delta^\alpha < 0 \\
& \Leftrightarrow \frac{\beta^\alpha \lambda^\alpha}{\mu^\alpha c^\alpha} N < 1 \\
& \stackrel{(4)}{\Leftrightarrow} \mathcal{R}_0 < 1,
\end{aligned}$$

then all eigenvalues have negative real part and X_0 is locally asymptotically stable. \square

3.4. CTL response-free and SARS-CoV-2 endemic equilibria. The following results show us that there is a region where a CTL response-free and SARS-CoV-2 endemic equilibria can coexist.

Lemma 3. *If $\mathcal{R}_0 > 1$, then the CTL response-free equilibrium point exists.*

Proof. If we impose $C = 0$ in the model (1) we get the following equilibrium point:

$$\begin{aligned}
X_1 &= (T_1, I_1, V_1, C_1) \\
&= \left(\frac{c^\alpha}{N\beta^\alpha}, \frac{N\beta^\alpha \lambda^\alpha - c^\alpha \mu^\alpha}{N\beta^\alpha \delta^\alpha}, \frac{N\beta^\alpha \lambda^\alpha - c^\alpha \mu^\alpha}{\beta^\alpha c^\alpha}, 0 \right).
\end{aligned}$$

It is clear that all cells and virus populations are non-negative. In this case it is easy to verify that $T_1 > 0$ and $C_1 = 0$. In order to I_1 and V_1 we have $(N\beta^\alpha \lambda^\alpha - c^\alpha \mu^\alpha)/(N\beta^\alpha \delta^\alpha) > 0$ and $(N\beta^\alpha \lambda^\alpha - c^\alpha \mu^\alpha)/(\beta^\alpha c^\alpha) > 0$, respectively. So, if

$$N\beta^\alpha \lambda^\alpha - c^\alpha \mu^\alpha > 0 \quad \Leftrightarrow \quad N\beta^\alpha \lambda^\alpha > c^\alpha \mu^\alpha \quad \stackrel{(4)}{\Leftrightarrow} \quad \mathcal{R}_0 > 1, \quad (6)$$

then $I_1, V_1 > 0$. Therefore, the CTL response-free equilibrium point exists. \square

Now, we set the following real constant will be useful in the upcoming results:

$$\varphi_0 = 1 + A, \quad (7)$$

where $A = \sigma^\alpha N\beta^\alpha \delta^\alpha / (q^\alpha c^\alpha \mu^\alpha)$. Since $A > 0$, then $\varphi_0 > 1$.

Lemma 4. *If $\mathcal{R}_0 > \varphi_0$, then the SARS-CoV-2 endemic and CTL response-free equilibria can coexist.*

Proof. Similar to Lemma 3, we compute the endemic equilibrium point of system (1) and we get

$$X_2 = (T_2, I_2, V_2, C_2),$$

where

$$\begin{aligned}
T_2 &= \frac{\lambda^\alpha c^\alpha q^\alpha}{\sigma^\alpha N \beta^\alpha \delta^\alpha + c^\alpha \mu^\alpha q^\alpha} \\
I_2 &= \frac{\sigma^\alpha}{q^\alpha} \\
V_2 &= \frac{N \delta^\alpha \sigma^\alpha}{q^\alpha c^\alpha} = \frac{N \delta^\alpha}{c^\alpha} I_2 \\
C_2 &= B \left[q^\alpha (N \beta^\alpha \lambda^\alpha - c^\alpha \mu^\alpha) - \sigma^\alpha N \beta^\alpha \delta^\alpha \right],
\end{aligned}$$

and $B = \delta^\alpha / [(\sigma^\alpha N \beta^\alpha \delta^\alpha + c^\alpha \mu^\alpha q^\alpha) k^\alpha] > 0$. It is clear that $T_2, I_2, V_2 > 0$. Since $B > 0$, if

$$q^\alpha (N \beta^\alpha \lambda^\alpha - c^\alpha \mu^\alpha) - \sigma^\alpha N \beta^\alpha \delta^\alpha > 0$$

$$\Leftrightarrow q^\alpha N \beta^\alpha \lambda^\alpha - q^\alpha c^\alpha \mu^\alpha - \sigma^\alpha N \beta^\alpha \delta^\alpha > 0$$

$$\Leftrightarrow q^\alpha (N \beta^\alpha \lambda^\alpha - c^\alpha \mu^\alpha) > \sigma^\alpha N \beta^\alpha \delta^\alpha$$

$$\Leftrightarrow N \beta^\alpha \lambda^\alpha - c^\alpha \mu^\alpha > \frac{\sigma^\alpha N \beta^\alpha \delta^\alpha}{q^\alpha}$$

$$\Leftrightarrow \frac{N \beta^\alpha \lambda^\alpha - c^\alpha \mu^\alpha}{c^\alpha \mu^\alpha} > \frac{\sigma^\alpha N \beta^\alpha \delta^\alpha}{q^\alpha c^\alpha \mu^\alpha}$$

$$\stackrel{(4)}{\Leftrightarrow} \mathcal{R}_0 > 1 + \frac{\sigma^\alpha N \beta^\alpha \delta^\alpha}{q^\alpha c^\alpha \mu^\alpha} \quad (8)$$

$$\stackrel{(7)}{\Leftrightarrow} \mathcal{R}_0 > \varphi_0, \quad (9)$$

then $C_2 > 0$. Hence, condition (9) provides the existence of the SARS-CoV-2 endemic equilibrium point. Moreover, looking at expressions (6) and (8), we can easily verify that the CTL response-free and SARS-CoV-2 endemic equilibria can coexist. Figure 1 illustrates this coexistence. \square

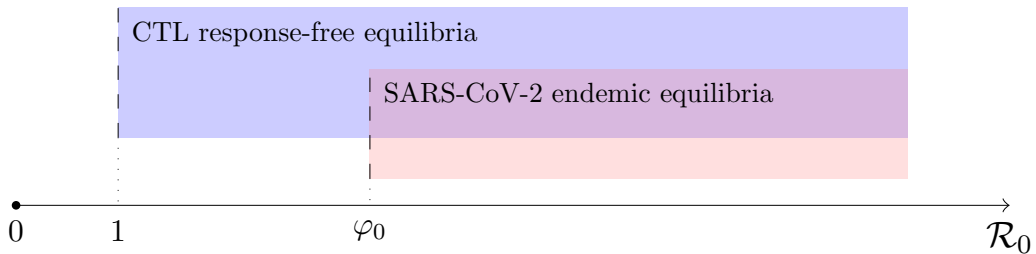


FIGURE 1. Coexistence space of SARS-CoV-2 endemic and CTL response-free equilibria for $\mathcal{R}_0 > \varphi_0$.

4. NUMERICAL SIMULATIONS AND RESULTS

In this section we simulate the variation of \mathcal{R}_0 as a function of β^α , μ^α , c^α , N and λ^α (see (4)) and sketched the dynamics of model (1) for different values of $\alpha \in [0, 1]$ and CTL proliferation functions. The parameter values used in the numerical simulations are in Table 2. The initial conditions that we assume are $T(0) = 1000$, $I(0) = 0$, $V(0) = 10$ and $C(0) = 333$ [35]. Since the model of the authors of [35] is similar to ours, we consider that these initial conditions also fit our model. The numerical solutions were obtained by applying the subroutine of Diethelm and Freed (FracPECE subroutine) [28].

Stability and convergence of the method. The classical Adams-Bashforth-Moulton method [36] used for first order differential equations is a good method and extremely useful in the sense that its stability properties provide safe information about in slightly stiff equations without glaring oscillations from rounding errors. We can find in [28] that these stability properties remain unchanged for differential equations of fractional order, that is, the stability of this method does not depend of the order of the fractional derivative α . Of course, stability alone is not sufficient in practice to make sure that the numerical solution is a good approximation to the exact solution. As such, convergence is a problem that must also be analysed. The method we use, is a method that uses the same techniques as [37] whose standard error is given by the expression

$$\max_j |y(t_j) - y_j| = O(h^2),$$

where $h = \max_j (t_{j+1} - t_j)$ and $t_j \in [t_0, t_0 + t^*]$ for some fixed $t^* > 0$. The FracPECE method was already used by other authors in previous studies, such as [14, 38].

Parameter	Symbol	Value	Reference
Proliferation rate of healthy cells	λ^α	10 cells mm ⁻³	[21]
SARS-CoV-2 infection rate	β^α	0.001 virions mm ³ day ^{-α}	[33]
Bursting size for virus growth	N	10 – 2500 virions cell ⁻¹	[21]
Proliferation rate of CTL	q^α	0.2	[21]
Elimination rate of infected cells by CTL	k^α	0.7 cells	[21]
Natural death rate of healthy cells	μ^α	0.01 day ^{-α}	[21]
Natural death rate of infected cells	δ^α	1 day ^{-α}	[34]
Natural death rate of CTL	σ^α	0.08 cells day ^{-α}	[21]
Death rate of virus	c^α	3 day ^{-α}	[21]
Level of saturation of CTL expansion	ε	0.01 cells	[21]
Half-saturation constant	a	120 cells	[21]

TABLE 2. Parameter values used in numerical simulations of model (1).

Figure 2 shows the behaviour of the four classes for different values of the fractional order derivative α . It is concluded that for lower α values there is a lower number of healthy T cells and CTL. However, and regarding the CTL, in the first 150 days, for low values of α there is a higher number of CTL. Also in the first 150 days, higher values of α relate to a lower number of CTL. We can also conclude that the lower the α value,

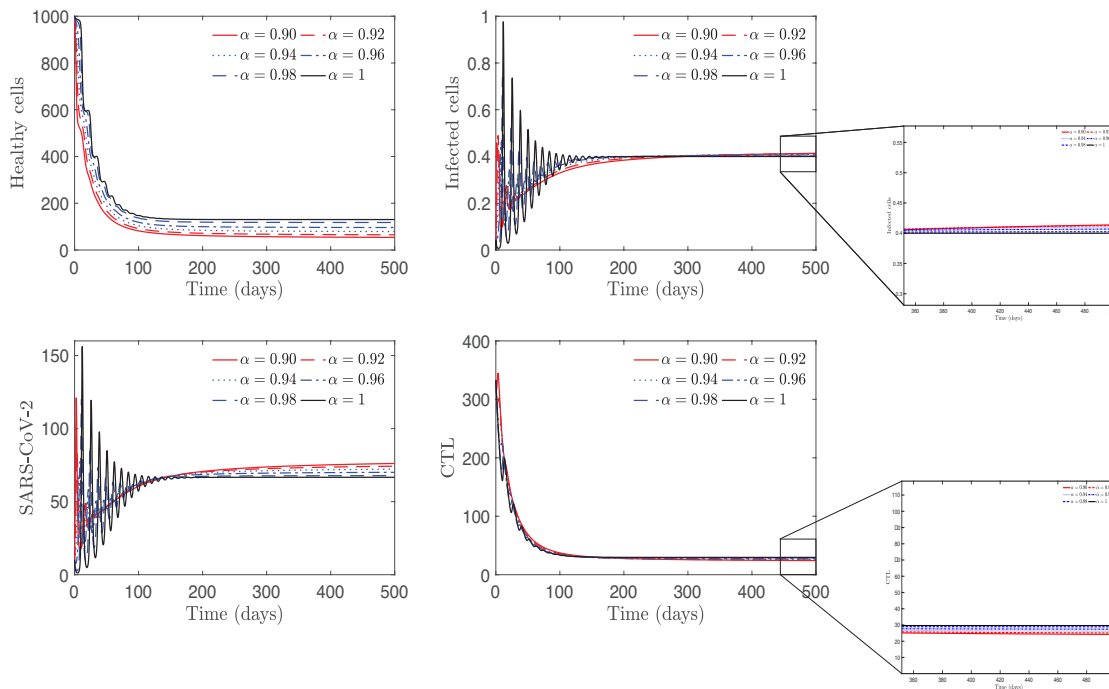


FIGURE 2. Dynamic behaviour of T , I , V and C populations for $\alpha \in \{0.90, 0.92, 0.94, 0.96, 0.98, 1\}$. We consider $f_n(I, C) = f_1(I, C)$. Initial conditions and parameter values are given in the text and in the Table 2, respectively.

the higher the viral load of SARS-CoV-2 in the organism. Regarding to infected cells, it is observed that the higher the α value, the lower the number of these cells.

Figures 3 – 6 show the effect of SARS-CoV-2 infection rate β^α , death rate of healthy cells μ^α , SARS-CoV-2 death rate c^α , bursting size for virus growth N , and proliferation rate of healthy cells λ^α , on the value of \mathcal{R}_0 , for $\alpha = 1$.

From literature in general, when $\mathcal{R}_0 < 1$ then the disease tends to slow down until it disappears. Otherwise, when $\mathcal{R}_0 > 1$, the disease spreads further and further through the population [32]. In all figures we can observe that \mathcal{R}_0 increases with the value of β , promoting the progression of SARS-CoV-2 infection. We can interpret the variation in this parameter value with the data from the World Health Organization (WHO) [3]. For example, during the periods when the governments of the countries allowed the population to be in lockdown, naturally the number of contacts increased and consequently the number of cases also increased. With this, at a cellular level, the viral load is higher and the transmission rate of SARS-CoV-2 between cells also increase. This behaviour was reflected in an increase of \mathcal{R}_0 , as we can see in Figures 3 – 6.

However, in Figure 3, for $\beta < 0.2$ or for $\mu > 0.25$, the *basic reproduction number* is less than 1, which leads us to conclude that the infection will eventually disappear. Figure 4 suggests that low values of β combined with high values of c result in a small value of \mathcal{R}_0 . We observed by Figure 5 that N has no apparent significant influence of the progression of SARS-CoV-2 infection. Furthermore, for $\beta < 0.15$ the infection tends to disappear. In Figure 6 we can see that \mathcal{R}_0 has lower values for combinations of low values of β and high values of λ .

In Figures 7 – 9 we consider four different immune functions $f_n(I, C)$, specifically $f_1(I, C) = q^\alpha IC$, $f_2(I, C) = q^\alpha I$, $f_3(I, C) = q^\alpha IC/(\varepsilon C + 1)$ and $f_4(I, C) = q^\alpha I/(a + \varepsilon I)$,

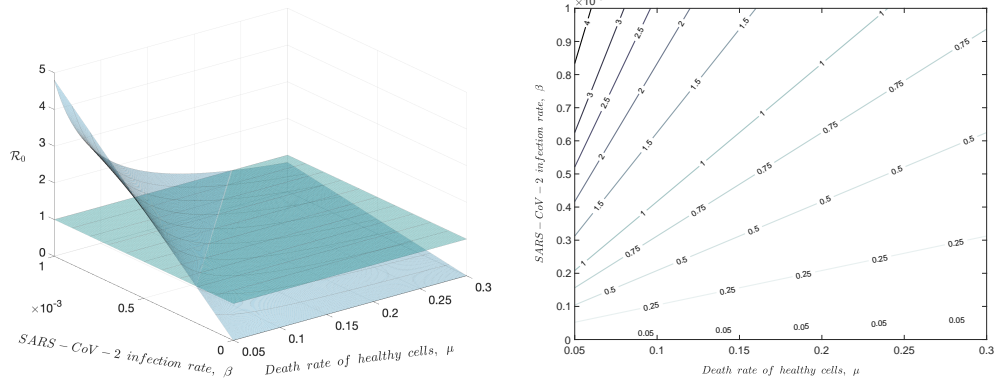


FIGURE 3. Effect of SARS-CoV-2 infection rate β , and death rate of healthy cells μ , on the *basic reproduction number* \mathcal{R}_0 . Initial conditions and parameter values are given in the text and in the Table 2, respectively, except for β and μ . We consider $\alpha = 1$.

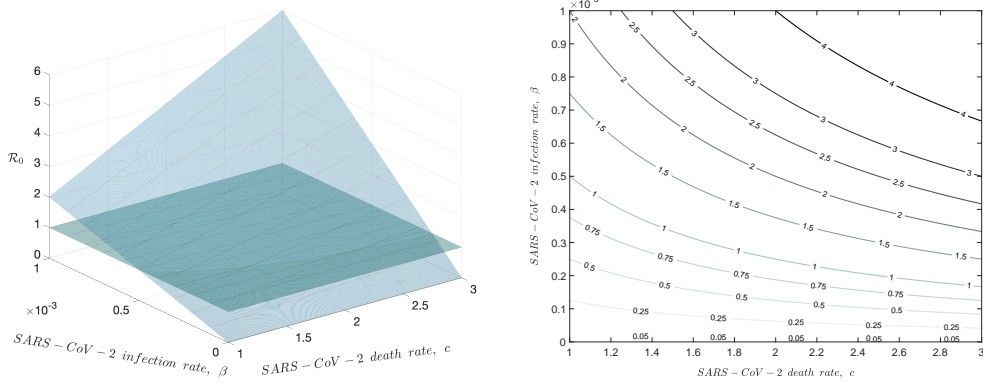


FIGURE 4. Effect of SARS-CoV-2 infection rate β and SARS-CoV-2 death rate c , on the *basic reproduction number* \mathcal{R}_0 . Initial conditions and parameter values are given in the text and in the Table 2, respectively, except for β and c . We consider $\alpha = 1$.

and different values of α (Please see figure legends). For all proliferation functions the system presents the same asymptotic behaviour converging to an endemic state. However, it can be observed that the number of infected cells and the SARS-CoV-2 viral load are higher when we consider the proliferation function f_4 . It is also possible to notice that for the proliferation function f_4 , there is a higher number of infected cells. This may be a consequence of the weak immune response (Please see CTL subplot). This weak immune response is also reflected in the viral load, which is also higher for f_4 . The opposite is true for f_1 . As the immune response is stronger, the number of infected cells and the viral load is lower. This dynamic occurs for all values of the order of the fractional derivative α , with the particularity that the lower its value, the less severe is the epidemic state.

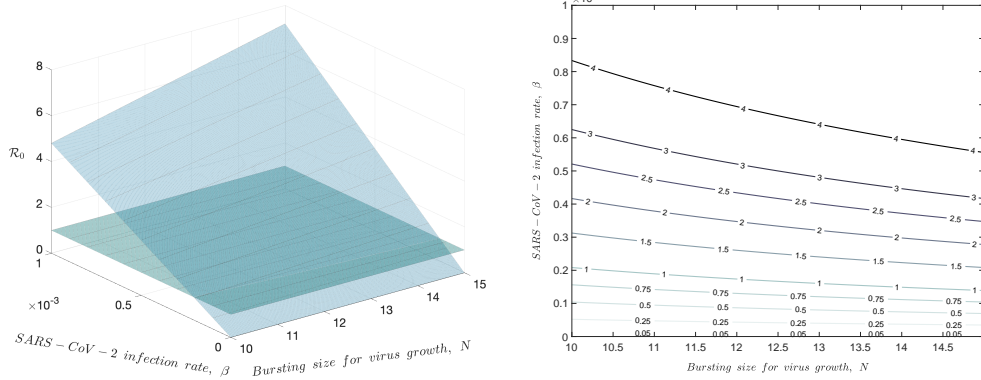


FIGURE 5. Effect of SARS-CoV-2 infection rate β , and bursting size for virus growth N , on the *basic reproduction number* \mathcal{R}_0 . Initial conditions and parameter values are given in the text and in the Table 2, respectively, except for β and N . We consider $\alpha = 1$.

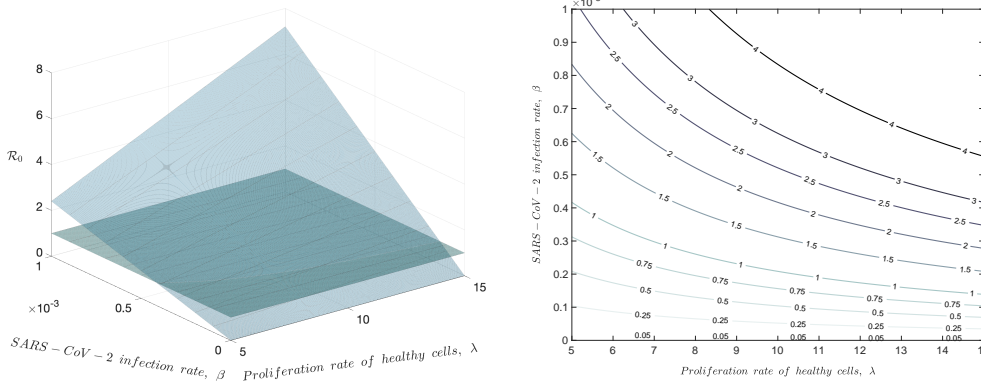


FIGURE 6. Effect of SARS-CoV-2 infection rate β , and proliferation rate of healthy cells λ , on the *basic reproduction number* \mathcal{R}_0 . Initial conditions and parameter values are given in the text and in the Table 2, respectively, except for β and λ . We consider $\alpha = 1$.

5. CONCLUSIONS

In this study, a FO model for the dynamics of SARS-CoV-2, responsible for CoViD-19, was analysed together with the human immune response, in particular CTL. The research essentially consisted of three key points:

- (I) Theoretical analysis of the model to find a region where two equilibria can co-exist;
- (II) Influence that the parameters of the model have on the progression of the virus within human organism;
- (III) Analysis of the immune response that human body is able to provide in the presence of SARS-CoV-2, for different α values.

Regarding the coexistence of two equilibria, we found that under particular conditions, namely for $\mathcal{R}_0 > \varphi_0$, the CTL response-free and SARS-CoV-2 endemic equilibria can coexist (see Figure 1). This result is quite important in that we find a range of values for the *basic reproduction number* ($1 < \mathcal{R}_0 < \varphi_0$) for which there is no disease or immune

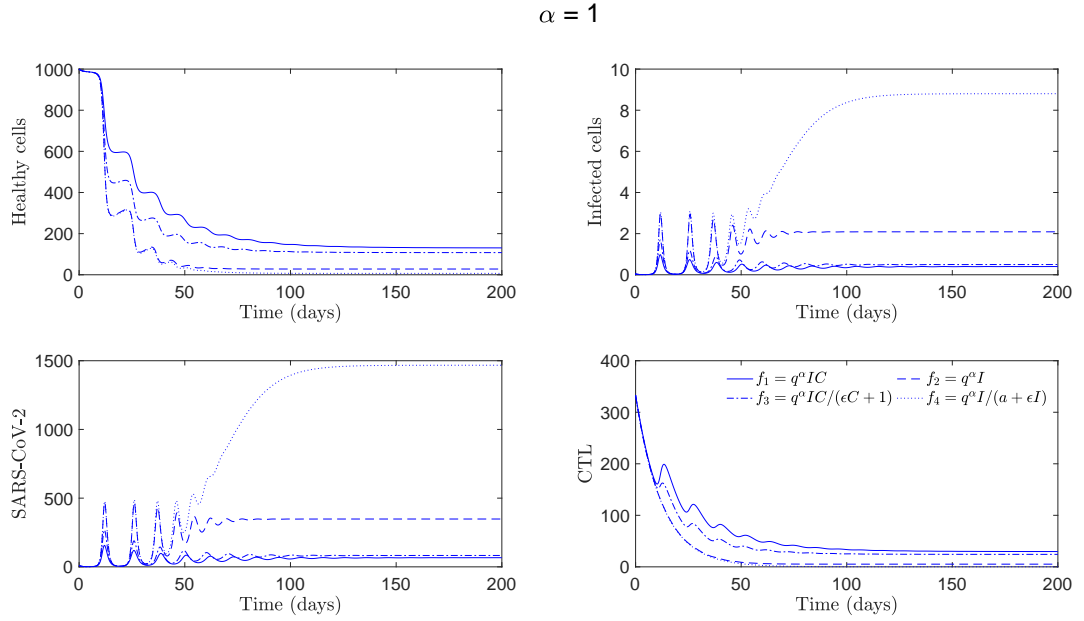


FIGURE 7. Dynamics of model (1) for f_1 , f_2 , f_3 and f_4 . Initial conditions and parameter values are given in the text and in the Table 2, respectively. We consider $\alpha = 1$.

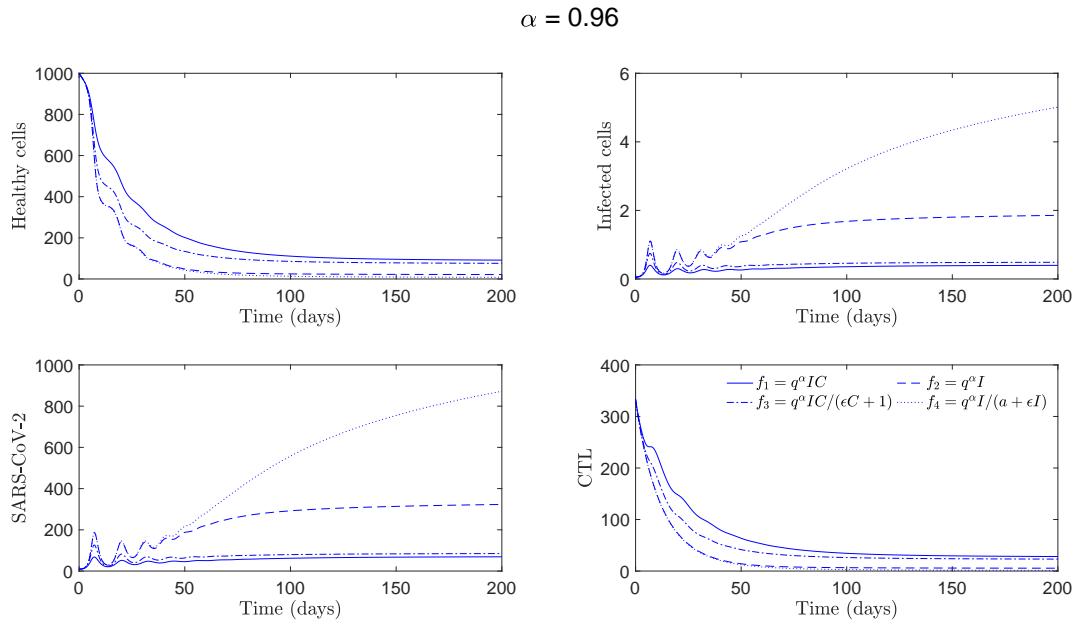


FIGURE 8. Dynamics of model (1) for f_1 , f_2 , f_3 and f_4 . Initial conditions and parameter values are given in the text and in the Table 2, respectively. We consider $\alpha = 0.96$.

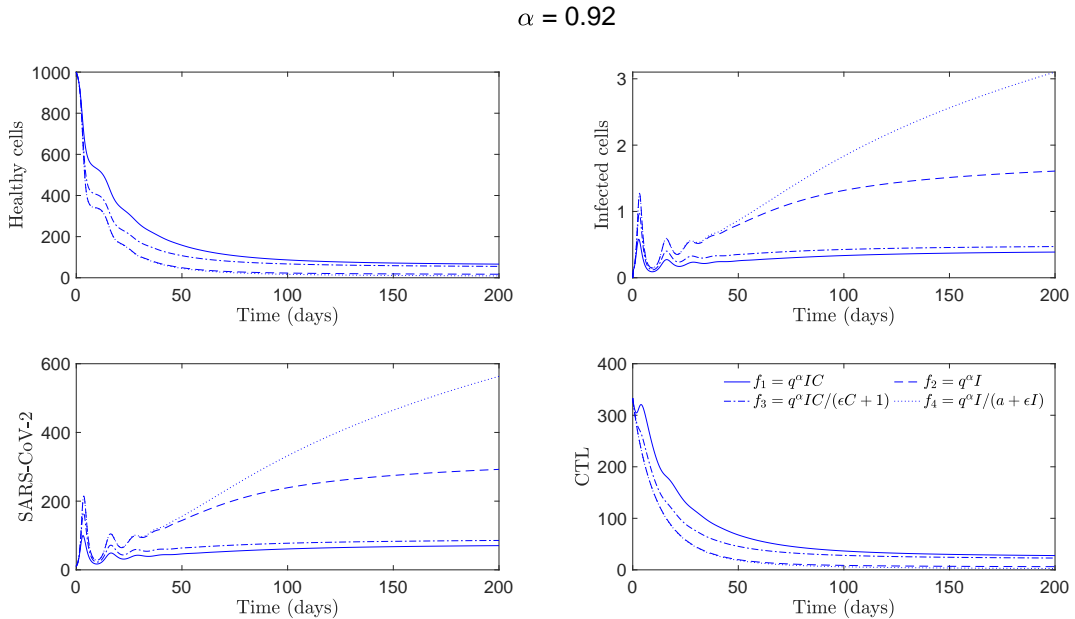


FIGURE 9. Dynamics of model (1) for f_1 , f_2 , f_3 and f_4 . Initial conditions and parameter values are given in the text and in the Table 2, respectively. We consider $\alpha = 0.92$.

response (which makes sense). However, for $\mathcal{R}_0 > \varphi_0$, the organism still has no immune response to the virus that is already present in the human body. This phenomenon should serve as a warning to health professionals and epidemiologists.

One of the conclusions that could possibly have more impact in real life is related to Figure 2. We can see that for lower values of α , the asymptotic behaviour of the populations stabilizes faster than for higher values of α . This scenario can play an important role in predicting cell behaviour earlier than if we run simulations with just the integer order derivative ($\alpha = 1$).

With respect to the *basic reproduction number* \mathcal{R}_0 , simulations have revealed that when $\beta < 0.2$, then $\mathcal{R}_0 < 1$, which leads us to conclude that the infection tends to disappear. So human body will be healthy again and free of infection.

With regard to the analysis of the immune response to infection, we simulated the model for four CTL proliferation functions:

$$f_1(I, C) = q^\alpha IC, \quad f_2(I, C) = q^\alpha I, \quad f_3(I, C) = \frac{q^\alpha IC}{\epsilon C + 1}, \quad f_4(I, C) = \frac{q^\alpha I}{a + \epsilon I},$$

using the subroutine of Diethelm and Freed [28].

We concluded that the *saturated type CTL production rate* f_4 , is the function that most worsens the endemic state of infection, although all CTL proliferation functions asymptotically converge towards an endemic equilibrium. Furthermore, we verified that CTL proliferation functions that trigger stronger immune responses, such as f_1 and f_3 , lead to fewer infected cells and a less pronounced viral load. All these conclusions about the immune response to SARS-CoV-2 are consistent for different values of α . However, the lower the value of α , the lower the endemic state of the infection.

The results of the simulations are in line with what was expected. The method we used to find numerical solutions to our model is a method that is used in many published

scientific papers, some of them on epidemic models similar to ours [35]. This leads us to believe that the accuracy of the numerical solutions of our model is quite reasonable. We address the readers who are interested in consulting the algorithm of Diethelm and Freed (1999) to reference [28].

These models allow us to draw a lot of conclusions about how we should act in situations related to epidemics in different countries around the world. For example, these mathematical analysis could help in decision making by government leaders in combating possible economic losses that come from pandemic disasters, particularly due to SARS-CoV-2 [14].

Considering the scarce information relating the dynamics of SARS-CoV-2 and the immune system, we were able to obtain solid results that may contribute to the understanding of the disease and its mechanisms of action from a mathematical point of view. We hope in the near future to present an improved version of this model, based on more biochemical information regarding parameter values. Additionally, we plan to include the effect of vaccination at a cellular level to study how the immune system is reinforced and what the impact is on other cells.

DECLARATIONS

Ethical statement. The authors have no ethical statement to declare

Funding. JPSMC was supported by CMUP, Portugal (UIDP/MAT/00144/2020), which is funded by Fundação para a Ciência e a Tecnologia (FCT)

Conflict of Interest/Competing interests. The authors declare that they have no conflict of interest

Availability of data and material. This manuscript has no associated data

Code availability. Not applicable

Authors' contributions. JPSMC is the only author of this work

REFERENCES

- [1] B. Hu, H. Guo, P. Zhou, Z. L. Shi, Characteristics of SARS-CoV-2 and COVID-19, *Nat. Rev. Microbiol.*, **19** (2021), 141–154
- [2] A. Vitiello, F. Ferrara, C. Pelliccia, G. Granata, R. La Porta, Cytokine storm and colchicine potential role in fighting SARS-CoV-2 pneumonia, *Ital. J. Med.* **14** (2020), 88–94
- [3] World Health Organization (WHO): <https://covid19.who.int> (2023). Accessed 12 May 2023
- [4] Worldometers: <https://www.worldometers.info/coronavirus/#countries> (2023). Accessed 12 May 2023
- [5] J. Sun, W. T. He, L. Wang, A. Lai, X. Ji, X. Zhai, G. Li, M. A. Suchard, J. Tian, J. Zhou, M. Veit, S. Su, COVID-19: Epidemiology, Evolution, and Cross-Disciplinary Perspectives, *Trends Mol. Med* **26** (2020), 483–495
- [6] H. A. Rothan, S. N. Byrareddy, The epidemiology and pathogenesis of coronavirus disease (COVID-19) outbreak, *J Autoimmun.* **109** (2020), 4 pages
- [7] D. Moriconi, S. Masi, E. Rebelos, A. Viridis, M. L. Manca, S. De Marco, S. Taddei, M. Nannipieri, Obesity prolongs the hospital stay in patients affected by COVID-19, and may impact on SARS-COV-2 shedding, *Obes. Res. Clin. Pract.* **14** (2020), 205–209
- [8] K. T. Bajgain, S. Badal, B. B. Bajgain, M.J. Santana, Prevalence of comorbidities among individuals with COVID-19: A rapid review of current literature, *Am. J. Infect. Control* **49** (2021), 238–246
- [9] C. Yi, Y. Yi, J. Li, mRNA Vaccines: Possible Tools to Combat SARS-CoV-2. *Viol. Sin.* **35** (2020), 259–262
- [10] K. J. Tracey, Vaccines Alone Are Not Enough to Beat COVID. Scientific American. <https://www.scientificamerican.com/article/vaccines-alone-are-not-enough-to-beat-covid/> (2021). Accessed 12 February 2021

- [11] L. Taylor, Why scientists worldwide are watching UK COVID infections, *Nature* **599** (2021), 189–190
- [12] L. L. Cunha, S. F. Perazzio, J. Azzi, P. Cravedi, L. V. Riella, Remodeling of the Immune Response With Aging: Immunosenescence and Its Potential Impact on COVID-19 Immune Response, *Front. Immunol.* **11** (2020), 11 pages
- [13] A. Sette, S. Crotty, Adaptive immunity to SARS-CoV-2 and COVID-19, *Cell* **184** (2021), 861–880
- [14] J.P.S. Maurício de Carvalho, B. Moreira-Pinto, A fractional-order model for CoViD-19 dynamics with reinfection and the importance of quarantine, *Chaos Solitons Fractals* **151** (2021),
- [15] Elie, R., Hubert, E. & Turinici, G. Contact rate epidemic control of COVID-19: an equilibrium view, *Math. Model. Nat. Phenom.* **15** (2021), 25 pages
- [16] M. Kočańczyk, F. Grabowski, T. Lipniacki, Dynamics of COVID-19 pandemic at constant and time-dependent contact rates, *Math. Model. Nat. Phenom.* **15** (2020), 12 pages
- [17] X. Liu, A simple, SIR-like but individual-based epidemic model: Application in comparison of COVID-19 in New York City and Wuhan, *Results Phys.* **20** (2021), 10 pages
- [18] I. Cooper, A. Monda, C. G. Antonopoulos, A SIR model assumption for the spread of COVID-19 in different communities, *Chaos Solitons Fractals* **139** (2020), 14 pages
- [19] S. Wang, Y. Pan, Q. Wang, H. Miao, A. N. Brown, L. Rong, Modeling the viral dynamics of SARS-CoV-2 infection, *Math. Biosci.* **328** (2020), 12 pages
- [20] A. N. Chatterjee, F. Al Basir, A Model for SARS-CoV-2 Infection with Treatment, *Comput. Math. Methods Med.* **2020** (2020), 11 pages
- [21] N. Bairagi, D. Adak, Dynamics of cytotoxic T-lymphocytes and helper cells in human immunodeficiency virus infection with Hill-type infection rate and sigmoidal CTL expansion, *Chaos Solitons Fractals* **103** (2017), 52–67
- [22] C. I. Muresan, A. Dutta, E. H. Dulf, Z. Pinar, A. Maxim, C. M. Ionescu, Tuning algorithms for fractional order internal model controllers for time delay processes, *Int. J. Control* **89** (2016), 579–593
- [23] N. H. Sweilam, M. M. A. Hasan, D. Baleanu, New studies for general fractional financial models of awareness and trial advertising decisions, *Chaos Solitons Fractals* **104** (2017), 772–784
- [24] D. Valério, J. J. Trujillo, M. Rivero, J. A. T. Machado, D. Baleanu, Fractional calculus: a survey of useful formulas, *Eur. Phys. J. Spec. Top.* **222** (2013), 1827–1846
- [25] K. Shah, M. Arfan, I. Mahariq, A. Ahmadian, S. Salahshour, M. Ferrara, Fractal-Fractional Mathematical Model Addressing the Situation of Corona Virus in Pakistan, *Results Phys.* **19** (2020), 12 pages
- [26] M. Awais, F. S. Alshammari, S. Ullah, M. A. Khan, S. Islam, Modeling and simulation of the novel coronavirus in Caputo derivative, *Results Phys.* **19** (2020), 9 pages
- [27] M. A. Aba Oud, A. Ali, H. Alrabaiah, S. Ullah, M. A. Khan, S. Islam, A fractional order mathematical model for COVID-19 dynamics with quarantine, isolation, and environmental viral load, *Adv. Differ. Equ.* **2021** (2021), 19 pages
- [28] K. Diethelm, A. D. Freed, The FracPECE Subroutine for the Numerical Solution of Differential Equations of Fractional Order. In: Heinzel S, Plessner T. (eds.) *orschung und wissenschaftliches Rechnen: Beitrage zum Heinz-Billing-Preis 1998*, (1999), pp. 57–71
- [29] S. Samko, A. Kilbas, O. Marichev, *Fractional integrals and derivatives: theory and applications*. London: Gordon and Breach Science Publishers (1993)
- [30] Z. M. Odibat, N. T. Shawagfeh, Generalized Taylor’s formula, *Appl. Math. Comput.* **186** (2007), 286–293
- [31] W. Lin, Global existence theory and chaos control of fractional differential equations, *J. Math. Anal. Appl.* **332** (2007), 709–726
- [32] van den Driessche, P. & Watmough, J. Reproduction numbers and sub-threshold endemic equilibria for compartmental models of disease transmission, *Math. Biosci.* **180** (2007), 29–48
- [33] S. Tang, W. Ma, P. Bai, A Novel Dynamic Model Describing the Spread of the MERS-CoV and the Expression of Dipeptidyl Peptidase 4, *Math. Methods Med.* **2017** (2017), 6 pages
- [34] A. Gonçalves, J. Bertrand, R. Ke, E. Comets, X. de Lamballerie, D. Malvy, A. Pizzorno, O. Terrier, M. R. Calatrava, F. Mentré, P. Smith, A. S. Perelson, J. Guedj, Timing of Antiviral Treatment Initiation is Critical to Reduce SARS-CoV-2 Viral Load, *CPT: Pharmacomet. Syst. Pharmacol.* **9** (2020), 509–514
- [35] A.R.M. Carvalho, C.M.A. Pinto, Immune response in HIV epidemics for distinct transmission rates and for saturated CTL response. *Math. Model. Nat. Phenom.* **14** (2019), 13 pages
- [36] E. Hairer, G. Wanner, *Solving Ordinary Differential Equations II: Stiff and Differential-Algebraic Problems*. Springer, Berlin (1996)
- [37] Linz, P. *Analytical and Numerical Methods for Volterra Equations*. SIAM, Philadelphia, PA (1985)

- [38] J.P.S. Maurício de Carvalho, C.M.A. Pinto, Role of the Immune System in AIDS-defining Malignancies. In: Awrejcewicz, J. (eds.) Perspectives in Dynamical Systems I: Mechatronics and Life Sciences. DSTA 2019. Springer Proceedings in Mathematics & Statistics, vol 362. Springer, Cham. (2022)